

# Solvent-Induced Frequency Shifts: Configuration Interaction Singles Combined with the Effective Fragment Potential Method

Pooja Arora,<sup>†</sup> Lyudmila V. Slipchenko,<sup>‡</sup> Simon P. Webb,<sup>§</sup> Albert DeFusco,<sup>†</sup> and Mark S. Gordon<sup>\*†</sup>

Department Of Chemistry and Ames Laboratory, Iowa State University, Ames, Iowa 50011, Department Of Chemistry, Purdue University, West Lafayette, Indiana 47907, and VeraChem LLC, PO Box 2206, Germantown, Maryland 20875

Received: February 27, 2010; Revised Manuscript Received: May 20, 2010

The simplest variational method for treating electronic excited states, configuration interaction with single excitations (CIS), has been interfaced with the effective fragment potential (EFP) method to provide an effective and computationally efficient approach for studying the qualitative effects of solvents on the electronic spectra of molecules. Three different approaches for interfacing a non-self-consistent field (SCF) excited-state quantum mechanics (QM) method and the EFP method are discussed. The most sophisticated and complex approach (termed fully self consistent) calculates the excited-state electron density with fully self-consistent accounting for the polarization (induction) energy of effective fragments. The simplest approach (method 1) includes a strategy that indirectly adds the EFP perturbation to the CIS wave function and energy via modified Hartree–Fock molecular orbitals, so that there is no direct EFP interaction with the excited-state density. An intermediate approach (method 2) accomplishes the latter in a noniterative perturbative manner. Theoretical descriptions of the three approaches are presented, and test results of solvent-induced shifts using methods 1 and 2 are compared with fully ab initio values. These comparisons illustrate that, at least for the test cases examined here, modification of the ground-state Hartree–Fock orbitals is the largest and most important factor in the calculated solvent-induced shifts. Method 1 is then employed to study the aqueous solvation of coumarin 151 and compared with experimental measurements.

## I. Introduction

The ability to predict and understand solvent-induced shifts in electronic spectra is of great importance in chemical, biological, and medicinal sciences.<sup>1–4</sup> Solvent-induced shifts in electronic spectra result from two sources, (a) intrinsic differences in the solute due to interactions with the field produced by solvent molecules and (b) differences between ground- and excited-state solute–solvent interactions due to modifications of the solute electron density by the surrounding solvent molecules. It has been demonstrated that excited-state properties of some solutes, such as coumarins, are very sensitive to interactions with surrounding solvent molecules.<sup>5–8</sup> Therefore, coumarins are widely used as a tool to investigate the solute–solvent interactions and solvation dynamics.<sup>4,9–12</sup> For example, recently, coumarin 153 has been used as a probe to study solvent dynamics in proteins by time-dependent fluorescence Stokes shift<sup>13</sup> measurements.<sup>14</sup> In order to understand the effects of polarity and the H-bonding of the solvents on the electronic spectrum of coumarin 120, a study by Zhao et al. using TDDFT<sup>15,16</sup> (time-dependent density functional theory) with the PCM<sup>17</sup> (polarizable continuum model) for solvents was performed.<sup>8</sup> By including the explicit solvent molecules that are hydrogen-bonded to the solute, these authors predicted that the intermolecular solute–solvent and solvent–solvent interactions at the microscopic level affect the transition energies of coumarin 120 in aqueous solution.

A study by Karelson et al. on solvent-induced shifts indicates that two explicit water molecules forming H-bonds with pyrimidine are necessary to accurately predict its solvent shift.<sup>18</sup> Similar conclusions were reached by Cave et al., who, using TDDFT combined with a dielectric continuum solvent model, showed that the excitation energies of coumarin 120 and coumarin 151 are overestimated compared to those from the experiments due to the lack of explicit descriptions of solute–solvent interactions in the solvent model.<sup>19</sup> Therefore, it is important to reliably model the solvent molecules and their impact on electronic spectra in order to capture the correct solvent-induced shifts in the absorption spectra.

Theoretical investigations of absorption spectra in the condensed phase are limited by difficulties in accurately incorporating the solvent environment into the quantum treatment of a solute system of interest. The treatment of the solvent molecules using ab initio methods would capture the solvent effects most accurately, but such treatments are limited by their computational demands. There have been some methodological advances for the study of condensed-phase electronic spectroscopy, especially using dielectric continuum methods to represent the solvents.<sup>18,20–27</sup> While continuum methods are computationally inexpensive, they cannot describe explicit solute–solvent interactions such as hydrogen bonding. In other words, the microscopic structure around the solute molecules is not adequately described by the implicit solvent methods. On the other hand, discrete solvent methods treat each solvent molecule explicitly, and the bulk behavior can also be described by using molecular dynamics and Monte Carlo simulation techniques. The disadvantage of the explicit solvent models is that they are dependent on the quality of the model potential and on the

\* To whom correspondence should be addressed.

<sup>†</sup> Iowa State University.

<sup>‡</sup> Purdue University.

<sup>§</sup> VeraChem LLC.

sampling of the configurational space. The latter is usually required to be extensive and therefore computationally demanding.

The present work introduces a discrete approach for analyzing solvent effects on electronic spectra, in which the singly excited configuration interaction (CIS) method is combined with the effective fragment potential (EFP)<sup>28,29</sup> method. The EFP, a model potential that is largely based on first principles, has been demonstrated to accurately reproduce the effects of solvents on electronically excited states. Yoo et al. combined the TDDFT method for excited states with EFP to study the optical properties of molecules in the condensed phase.<sup>30</sup> This TDDFT/EFP investigation successfully reproduced the experimentally observed solvent-induced shifts of acetone. While the present work focuses on the simple CIS method, the strategies that are presented here are relevant for most *ab initio* excited-state methods.

Several theoretical methods are routinely employed for determining excited-state properties in the gas and condensed phases. These include CIS,<sup>31–33</sup> TDDFT,<sup>15,16,32</sup> complete active space self-consistent field (CASSCF),<sup>34–37</sup> configuration interaction with single and double excitations (CISD),<sup>38</sup> symmetry-adapted cluster configuration interaction (SAC-CI),<sup>39,40</sup> equation-of-motion coupled-cluster (EOM-CC),<sup>41–43</sup> multireference perturbation theory (MRPT),<sup>44,45</sup> and multireference CI (MRCI).<sup>46,47</sup> CIS is the simplest and least computationally demanding of these methods. It provides a qualitatively correct characterization of excited states that are dominated by single excitations.

There are two versions of the EFP method. EFP1 is specific to water and has been implemented for Hartree–Fock (HF) and density functional theory (DFT). EFP2 is a more general method that has not yet been fully interfaced with *ab initio* methods. The focus of the present work is to combine CIS with the EFP1/HF method to calculate solvent-induced shifts in the UV spectra of solute molecules. Three approaches are considered, all of which are relevant as well to most of the excited-state methods mentioned in the previous paragraph and to EFP1/DFT as well. Only minor modifications will be required for the more general EFP2 method,<sup>28,48,49</sup> once that method has been fully interfaced with *ab initio* methodology.

An important contribution to solvent-induced spectral shifts is the induction (polarization) energy because the electron density of the solute changes upon excitation, and the polarization of the solvent will respond to the altered electron density in its excited state. Some studies have considered the importance of mutual solute–solvent polarization between solute and solvent molecules on the excitation energy.<sup>46,50,51</sup> Xu et al. examined the effects of solute polarization of the  $n-\pi^*$  transition of formaldehyde in the condensed phase using a QM/MM method that combines MRCI and molecular dynamics simulations using a classical force field.<sup>46</sup> They found that the solute polarizability is an important component of solvent-induced shifts of formaldehyde, contributing about 35% of the shift in the calculated excitation energy. Aidas et al. have found that the inclusion of explicit polarization due to solvent molecules in combined quantum mechanics/molecular mechanics (QM/MM) calculations of excited states slightly lowers the excitation energy.<sup>50</sup> Studies by Kongsted et al. combined the coupled-cluster method with a MM method and introduced polarization effects due to solvent molecules using an iterative self-consistent approach. These authors found that neglecting the MM polarization overestimated the excitation energies.<sup>51</sup>

Several studies on electronic spectroscopy in the condensed phase have combined a QM method with explicit solvent models that incorporate polarization effects. Luzhkov et al. developed

a hybrid QM/MM method to study the solvent effects on electronic spectra using a Langevin dipole<sup>52</sup> solvent model.<sup>53</sup> Another study by Thompson et al. described a QM method combined with a polarizable MM method to study excited states.<sup>54</sup> Gao et al. implemented a combined QM–polarizable MM potential approach for excited states to examine the solvent effects on pyrimidine.<sup>55</sup> They used a semiempirical method for the solute and a classical model for the solvent molecules. Karelson and co-workers successfully extended the SCRf (self-consistent reaction field)<sup>56</sup> implicit model to study solvent effects on excited states including solvent polarization.<sup>24</sup> As outlined in the next section, a key feature of the EFP method is that it includes a solvent polarization term that is iterated to self-consistency within the quantum mechanical part of the calculation. The EFP solvent model poses an advantage over continuum models by being an explicit and polarizable solvent model that can describe the instantaneous electronic response of the solvent molecules for electronic excitations.

In the present study, three approaches to the CIS/EFP1 QM/MM method are presented. In the most sophisticated and complex approach (termed fully self consistent), the polarization (induction) term of EFP is fully iterated to be self-consistent with the excited-state wave function. This method provides an excited state that is fully consistent with the environment by calculating the response of the environment according to the electron density of the excited state, within the CIS iterative (Davidson diagonalization<sup>57</sup>) procedure. The second approach (method 1) is the simplest way to indirectly add the polarization perturbation to the excited state via modified HF orbitals. The third approach (method 2) is a compromise between the first two, in which the calculation of the excited-state solvent response within the CIS iterative procedure is avoided by employing a one-time perturbative correction term that estimates the solvent response for the excited-state density.

The outline of this paper is as follows. In section II, the methodological details of the three approaches for interfacing the CIS and EFP1/HF methods are described. Section III describes the computational details. Section IV benchmarks and illustrates the accuracy of the CIS/EFP1 schemes for several small molecules. Applications of the CIS/EFP1 interface to acetone and coumarin 151 using a molecular dynamics simulation are also presented. Conclusions are drawn in section V.

## II. Theory

**A. Summary of the EFP Method.** The effective fragment potential method has been described in many previous papers;<sup>28,29</sup> therefore, it is only briefly summarized here. The version of the EFP method used in the present work is based in part on the Hartree–Fock (HF) method and is referred to as EFP1/HF. However, the entire discussion is equally applicable to the analogous method that was derived from DFT, EFP1/DFT.<sup>58</sup> EFP1/HF contains three terms that describe solute–solvent and solvent–solvent Coulombic, induction, and exchange repulsion interactions. Coulomb (electrostatic) interactions in the EFP method are represented by a distributed multipole analysis (DMA) up through octopoles.<sup>59</sup> The electrostatic EFP contribution to the QM Hamiltonian is<sup>28</sup>

$$V_k^{es}(m, s) = \sum_{k=1}^{N_k} \left[ -\frac{q_k}{r_k} - \sum_a^{x,y,z} \mu_a^k \hat{F}_a(r_k) - \frac{1}{3} \sum_{ab}^{x,y,z} \Theta_{ab}^k \hat{F}_{ab}(r_k) - \frac{1}{15} \sum_{abc}^{x,y,z} \Omega_{abc}^k \hat{F}_{abc}(r_k) \right] \quad (1)$$

where  $\mu$ ,  $\Theta$ , and  $\Omega$  are the EFP dipole, quadrupole, and octopole moments, respectively.  $\hat{F}_a$ ,  $\hat{F}_{ab}$ , and  $\hat{F}_{abc}$  are the solute electric field, field gradient, and second derivative field operators, respectively.  $N_k$  is the total number of EFP multipole expansion points. A damping term is used to account for the overlapping charge densities when the solute–solvent or solvent–solvent molecules are very close to each other.<sup>60</sup>

The polarization (induction) term is treated using a finite field dipole–induced dipole model in which the interaction is iterated to self-consistency. In the EFP approach, the polarizability tensor is expressed in terms of individual localized molecular orbital (LMO) tensors for each LMO in the molecule, for example, two bond LMOs and two lone pair LMOs in water. The polarization/induction contribution to the QM Hamiltonian is given in eq 2.  $F$  is the field due to the ab initio part of the system, and  $\tilde{\alpha}_{ab}^l(m)$  is the polarizability component of the  $m$ th fragment in the  $l$ th localized orbital;  $a$  and  $b$  run over the  $x$ ,  $y$ ,  $z$  coordinates

$$V_l^{\text{pol}} = -\frac{1}{2} \sum_{a,b}^{x,y,z} F_a(r_1) \tilde{\alpha}_{ab}^l(m) \langle F_b(r_1) \rangle \quad (2)$$

The third EFP term is a remainder term that accounts for all interactions that are not accounted for in the first two terms. At the Hartree–Fock (HF) level of theory, these are the exchange repulsion + charge transfer interactions. For QM-EFP interactions, the remainder term is expanded in terms of Gaussian functions

$$V_m^{\text{rem}} = \sum_j \beta_{m,j} \exp(-\alpha_{m,j} r_m^2) \quad (3)$$

where  $m$  refers to a fragment center for the exchange repulsion potential. The expansion points are the atomic centers and the center of mass. The parameter  $\beta$  is generally set equal to unity, and the expansion includes only one term. The parameters  $\alpha$  are obtained by evaluating the HF water dimer potential at many points, subtracting the Coulomb and induction interactions, and fitting the QM-EFP remainder term to the remaining HF interaction.<sup>28</sup> The corresponding EFP-EFP remainder interaction is obtained in a similar manner, except that exponential functions are used rather than Gaussians.

**B. EFP-QM Interface.** In the present study, the solvent effects are treated using the effective fragment potential (EFP) method. The aim is to calculate the vertical excitations, with and without the presence of solvent molecules, at the optimized ground-state geometry, in order to assess the affects of the solvent on the calculated excitation energies. Because of the dependence of the EFP induction interaction on the solute electron density, the changing electron density of the solute upon electronic excitation must be accounted for by iterating the dipole–induced dipole interaction to self-consistency. In order to accomplish this, three approaches have been developed, as summarized in the following paragraphs.

**Fully Self-Consistent Method.** This method is the most rigorous approach for combining the EFP1/HF method with a QM method for excited states. It involves a coupled iterative procedure that solves both the solute wave function (represented by CIS) and the solvent-induced dipoles (represented by EFP1/HF) to obtain an excited state that is fully consistent with the environment. Since this method adds the polarization perturbation in a self-consistent manner within the CIS Davidson

diagonalization iterative procedure, it is the most accurate and complete description of the inclusion of polarization perturbation in the excited-state energy.

The total Hamiltonian of the excited-state system can be written as

$$H^{\text{EX}} = H_o^{\text{EX}} + H_{\text{pol}}^{\text{EX}} \quad (4)$$

The superscript EX represents the excited state.

$H_{\text{pol}}^{\text{EX}}$  in eq 4 is the EFP1 polarization interaction term.  $H_o^{\text{EX}}$  is

$$H_o^{\text{EX}} = H_{\text{oo}}^{\text{EX}} + H_{\text{es}}^{\text{EX}} + H_{\text{rem}}^{\text{EX}} \quad (5)$$

$H_{\text{oo}}^{\text{EX}}$  in eq 5 is the gas-phase time-independent QM Hamiltonian of the system.  $H_{\text{es}}^{\text{EX}}$  represents the electrostatic interaction term, and  $H_{\text{rem}}^{\text{EX}}$  is the exchange repulsion + charge transfer EFP interaction term.

The total excited-state energy of the system is given as follows

$$E^{\text{EX}} = \langle \psi_{\text{CIS}} | H_o^{\text{EX}} + H_{\text{pol}}^{\text{EX}} | \psi_{\text{CIS}} \rangle \quad (6)$$

where  $\psi_{\text{CIS}}$  is the CIS wave function.

The polarization/induction interaction must be iterated to self-consistency. In order to derive the polarization contribution to the excited-state energy, consider the polarization energy expression in terms of induced dipoles that is analogous to the ground-state expression obtained by Day et al.<sup>29</sup>

$$E_{\text{pol}}^{\text{EX}} = -\frac{1}{2} \sum_i (\bar{\mu}_i^{\text{EX}} - \bar{\mu}_i^{\text{EX}'}) \bar{F}_i^{\text{tot,EX}} \quad (7)$$

The quantities in eq 7 are defined as follows;  $\bar{\mu}_i^{\text{EX}}$  is the total induced dipole moment vector at the polarizable point  $i$  in the EFP. The polarizable points are taken to be the centroids of the localized molecular orbitals in the effective fragment. The induced dipole moments may be written in terms of the polarizability  $\tilde{\alpha}_i$  at polarizable point  $i$ , and the total field  $\bar{F}_i^{\text{tot,EX}}$ :

$$\bar{\mu}_i^{\text{EX}} = \tilde{\alpha}_i \bar{F}_i^{\text{tot,EX}}$$

$\bar{\mu}_i^{\text{EX}'}$  in eq 7 is the dipole moment induced by the field of the induced dipoles and is written as

$$\mu_i^{\text{EX}'} = \tilde{\alpha}_i^T \bar{F}_i^{\mu,\text{EX}}$$

where  $\tilde{\alpha}_i^T$  is the transpose of the polarizability tensor. The total field  $\bar{F}_i^{\text{tot,EX}}$  in eq 7 at the polarizable point  $i$  contains four components and is written as

$$\bar{F}_i^{\text{tot,EX}} = \bar{F}_i^{\text{nuc}} + \langle \psi_{\text{CIS}} | \bar{J}_i^{\text{el}} | \psi_{\text{CIS}} \rangle + \bar{F}_i^{\text{efp}} + \bar{F}_i^{\mu,\text{EX}} \quad (8)$$

where,  $\bar{F}_i^{\text{nuc}}$  and  $\langle \psi_{\text{CIS}} | \bar{J}_i^{\text{el}} | \psi_{\text{CIS}} \rangle$  are the fields from the QM nuclei and from the electrons, respectively

$\bar{F}_i^{\text{efp}}$  represents the field due to the static multipoles on the EFP fragments, and  $\bar{F}_i^{\mu,\text{EX}}$  is the field vector from induced dipoles on the EFP fragments.

The contribution from the polarization energy in the excited state can be obtained using the variational method. The functional can be formed as

$$L = E^{\text{EX}} - W^{\text{EX}}(\langle\psi_{\text{CIS}}|\psi_{\text{CIS}}\rangle - 1) \quad (9)$$

where  $W^{\text{EX}}$  is the Lagrange multiplier due to the normalization constraint. Also,  $E^{\text{EX}}$  represents the energy that is obtained directly from quantum mechanics and contains the polarization contribution.

Equations 6–9 lead to

$$L = E_o^{\text{EX}} - \frac{1}{2} \sum_i (\bar{\mu}_i^{\text{EX}} - \bar{\mu}_i^{\text{EX}'}) \bar{F}_i^{\text{tot,EX}} - W^{\text{EX}}(\langle\psi_{\text{CIS}}|\psi_{\text{CIS}}\rangle - 1) \quad (10)$$

where  $E_o^{\text{EX}} = \langle\psi_{\text{CIS}}|H_o^{\text{EX}}|\psi_{\text{CIS}}\rangle$ .

$$L = E_o^{\text{EX}} - \frac{1}{2} \sum_i (\bar{\alpha}_i \bar{F}_i^{\text{tot,EX}}) \bar{F}_i^{\text{tot,EX}} + \frac{1}{2} \sum_i (\bar{\alpha}_i^T \bar{F}_i^{\mu,\text{EX}}) \bar{F}_i^{\text{tot,EX}} - W^{\text{EX}}(\langle\psi_{\text{CIS}}|\psi_{\text{CIS}}\rangle - 1) \quad (11)$$

Recall that  $H_o^{\text{EX}}$  contains the contributions from the EFP Coulomb and remainder interactions. Variation of eq 11 with respect to the wave function parameters gives the following

$$\delta L = \delta E_o^{\text{EX}} - \frac{1}{2} \sum_i [(\bar{\alpha}_i + \bar{\alpha}_i^T) \bar{F}_i^{\text{tot,EX}} - \bar{\alpha}_i^T \bar{F}_i^{\mu,\text{EX}}] \delta \langle\psi_{\text{CIS}}|\bar{f}_i^{\text{el}}|\psi_{\text{CIS}}\rangle - W^{\text{EX}} \delta \langle\psi_{\text{CIS}}|\psi_{\text{CIS}}\rangle \quad (12)$$

Applying the condition  $\delta L = 0$  to eq 12 gives

$$\langle\delta\psi_{\text{CIS}}|H_o^{\text{EX}}|\psi_{\text{CIS}}\rangle - \frac{1}{2} \sum_i [(\bar{\mu}_i^{\text{EX}} + \bar{\mu}_i^{\text{EX}\pm} - \bar{\mu}_i^{\text{EX}'})] \langle\delta\psi_{\text{CIS}}|\bar{f}_i^{\text{el}}|\psi_{\text{CIS}}\rangle - W^{\text{EX}}(\langle\delta\psi_{\text{CIS}}|\psi_{\text{CIS}}\rangle) + \text{cc} = 0 \quad (13)$$

where cc stands for complex conjugate and  $\bar{\mu}_i^{\text{EX}\pm} = \bar{\alpha}_i^T \bar{F}_i^{\text{tot,EX}}$ .  $\bar{\mu}_i^{\text{EX}}$  and  $\bar{\mu}_i^{\text{EX}\pm}$  in eq 13 are equal if the polarizability tensor is symmetric ( $\bar{\alpha}_i^T = \bar{\alpha}_i$ ).  $W^{\text{EX}}$  is

$$W^{\text{EX}} = \langle\psi_{\text{CIS}}|H_o^{\text{EX}} - \frac{1}{2} \sum_i [(\bar{\mu}_i^{\text{EX}} + \bar{\mu}_i^{\text{EX}\pm}) \bar{f}_i^{\text{el}}] + \frac{1}{2} \sum_i \bar{\mu}_i^{\text{EX}'} \bar{f}_i^{\text{el}} |\psi_{\text{CIS}}\rangle \quad (14)$$

$$W^{\text{EX}} = E_o^{\text{EX}} - \frac{1}{2} \sum_i (\bar{\mu}_i^{\text{EX}} + \bar{\mu}_i^{\text{EX}\pm} - \bar{\mu}_i^{\text{EX}'}) \langle\psi_{\text{CIS}}|\bar{f}_i^{\text{el}}|\psi_{\text{CIS}}\rangle \quad (15)$$

Equation 14 represents the Hamiltonian matrix containing the contribution from the polarization perturbation in the form of induced dipoles. In order to obtain the final converged CIS eigenvalues and eigenvectors, one of two approaches could be employed; (a) an ideal way to add the polarization perturbation

in the CIS Hamiltonian would be to use the relaxed excited-state density (expectation value density + non-Hellman Feynman contribution),<sup>61</sup> This would require solving multiple coupled-perturbed Hartree–Fock (CPHF) equations<sup>62,63</sup> to iterate on the relaxed excited state density and the corresponding induced dipoles. (b) Alternatively, one could form the nonrelaxed excited-state density (ignoring the non-Hellman Feynman term) and the corresponding induced dipoles and iterate only within the Davidson diagonalization procedure to obtain the final eigenvectors and eigenvalues. Obtaining an excited state that is fully consistent with the environment using either of these two approaches is likely to be computationally demanding.<sup>64</sup>

The variational procedure does not produce the complete energy; therefore, the total energy is

$$E^{\text{EX}} = E_o^{\text{EX}} + E_{\text{pol}}^{\text{EX}} \quad (16)$$

Substituting  $E_o^{\text{EX}}$  from eq 15 and  $E_{\text{pol}}^{\text{EX}}$  from eq 7 to form  $E^{\text{EX}}$

$$E^{\text{EX}} = W^{\text{EX}} + \left( \frac{1}{2} \sum_i (\bar{\mu}_i^{\text{EX}} + \bar{\mu}_i^{\text{EX}\pm} - \bar{\mu}_i^{\text{EX}'}) \langle\psi_{\text{CIS}}|\bar{f}_i^{\text{el}}|\psi_{\text{CIS}}\rangle - \frac{1}{2} \sum_i (\bar{\mu}_i^{\text{EX}} - \bar{\mu}_i^{\text{EX}'}) \bar{F}_i^{\text{tot,EX}} \right) \quad (17)$$

The second term in eq 17 is the correction term to the quantum mechanical energy,  $W^{\text{EX}}$ , that is necessary in order to obtain the correct total energy.

The ground-state energy obtained using the same procedure as in eqs 6–17 is

$$E^{\text{G}} = W^{\text{G}} + \left( \frac{1}{2} \sum_i (\bar{\mu}_i^{\text{G}} + \bar{\mu}_i^{\text{G}\pm} - \bar{\mu}_i^{\text{G}'}) \langle\psi|\bar{f}_i^{\text{el}}|\psi\rangle - \frac{1}{2} \sum_i (\bar{\mu}_i^{\text{G}} - \bar{\mu}_i^{\text{G}'}) \bar{F}_i^{\text{tot,G}} \right) \quad (18)$$

where the superscript G represents the ground state and  $\bar{\mu}_i^{\text{G}}$ ,  $\bar{\mu}_i^{\text{G}\pm}$ , and  $\bar{\mu}_i^{\text{G}'}$  are the ground-state induced dipoles.  $\psi$  is the ground-state wave function.  $W^{\text{G}}$  is the quantum mechanical energy of the ground state that contains the polarization contribution from EFP and is obtained via the variational procedure.

The transition energy for the fully self-consistent method can be obtained as

$$\Delta E = E^{\text{EX}} - E^{\text{G}} \quad (19)$$

$$\Delta E = W^{\text{EX}} + \left( \frac{1}{2} \sum_i (\bar{\mu}_i^{\text{EX}} + \bar{\mu}_i^{\text{EX}\pm} - \bar{\mu}_i^{\text{EX}'}) \langle\psi_{\text{CIS}}|\bar{f}_i^{\text{el}}|\psi_{\text{CIS}}\rangle - \frac{1}{2} \sum_i (\bar{\mu}_i^{\text{EX}} - \bar{\mu}_i^{\text{EX}'}) \bar{F}_i^{\text{tot,EX}} \right) - W^{\text{G}} - \left( \frac{1}{2} \sum_i (\bar{\mu}_i^{\text{G}} + \bar{\mu}_i^{\text{G}\pm} - \bar{\mu}_i^{\text{G}'}) \langle\psi|\bar{f}_i^{\text{el}}|\psi\rangle - \frac{1}{2} \sum_i (\bar{\mu}_i^{\text{G}} - \bar{\mu}_i^{\text{G}'}) \bar{F}_i^{\text{tot,G}} \right) \quad (20)$$

Equation 17 is the final equation for the excited-state energy for the fully self-consistent method that includes iterating excited-state induced dipoles to self-consistency within the CIS iterative procedure. This procedure, while possibly tractable for CIS, would be very time-consuming for complex methods such

as multireference CI, multireference perturbation theory, CISD, or EOM-CC.<sup>41</sup> Now, consider two approximations to the fully self-consistent method.

**Method 1.** The simplest approach is to include the polarization effect due to the EFP solvent molecules only in the ground-state HF orbitals. The excited states are then altered because the HF orbitals have been modified, and these modified MOs in turn alter the CI coefficients. There is no direct modification of the CI coefficients.

The total excited-state energy for method 1 including the EFP1 perturbation is given as

$$E_1^{\text{EX}} = \langle \psi_{\text{CIS}} | H_0^{\text{EX}} + H_{\text{pol}}^{\text{G}} | \psi_{\text{CIS}} \rangle \quad (21)$$

The numerical subscript in eq 21, and in equations hereafter, indicates the method number (1 or 2).

$H_0^{\text{EX}}$  is the Hamiltonian operator for the ab initio part plus the contribution from the EFP1 exchange repulsion + charge transfer and electrostatic terms.

Similar to the fully self-consistent method, the variational procedure is applied to method 1, and the functional is

$$L = E_1^{\text{EX}} - W_1^{\text{EX}} (\langle \psi_{\text{CIS}} | \psi_{\text{CIS}} \rangle - 1) \quad (22)$$

Following the same procedure as in eqs 6–17, the QM energy containing the contribution from the polarization perturbation can be obtained as

$$W_1^{\text{EX}} = \langle \psi_{\text{CIS}} | \left( H_0^{\text{EX}} - \frac{1}{2} \sum_i (\bar{\mu}_i^{\text{G}} - \bar{\mu}_i^{\text{G}'}) \bar{f}_i^{\text{el}} \right) | \psi_{\text{CIS}} \rangle \quad (23)$$

$$W_1^{\text{EX}} = E_0^{\text{EX}} - \frac{1}{2} \sum_i (\bar{\mu}_i^{\text{G}} - \bar{\mu}_i^{\text{G}'}) \langle \psi_{\text{CIS}} | \bar{f}_i^{\text{el}} | \psi_{\text{CIS}} \rangle \quad (24)$$

The total excited-state energy is then

$$E_1^{\text{EX}} = E_0^{\text{EX}} + E_{\text{pol}}^{\text{G}} \quad (25)$$

where the polarization energy,  $E_{\text{pol}}^{\text{G}}$ , as derived for the ground state, is

$$E_{\text{pol}}^{\text{G}} = -\frac{1}{2} \sum_i (\bar{\mu}_i^{\text{G}} - \bar{\mu}_i^{\text{G}'}) \bar{F}_i^{\text{tot,G}} \quad (26)$$

$$E_1^{\text{EX}} = W_1^{\text{EX}} + \frac{1}{2} \sum_i (\bar{\mu}_i^{\text{G}} - \bar{\mu}_i^{\text{G}'}) \langle \psi_{\text{CIS}} | \bar{f}_i^{\text{el}} | \psi_{\text{CIS}} \rangle - \frac{1}{2} \sum_i (\bar{\mu}_i^{\text{G}} - \bar{\mu}_i^{\text{G}'}) \bar{F}_i^{\text{tot,G}} \quad (27)$$

Equation 27 is the final working equation for the total excited-state energy for method 1. The transition energy is

$$\Delta E = E_1^{\text{EX}} - E^{\text{G}} \quad (28)$$

Using eqs 27 and 18, one obtains the following for the excitation energy:

$$\Delta E = \left( W_1^{\text{EX}} + \frac{1}{2} \sum_i (\bar{\mu}_i^{\text{G}} - \bar{\mu}_i^{\text{G}'}) \langle \psi_{\text{CIS}} | \bar{f}_i^{\text{el}} | \psi_{\text{CIS}} \rangle - \frac{1}{2} \sum_i (\bar{\mu}_i^{\text{G}} - \bar{\mu}_i^{\text{G}'}) \bar{F}_i^{\text{tot,G}} \right) - \left( W^{\text{G}} + \frac{1}{2} \sum_i (\bar{\mu}_i^{\text{G}} + \bar{\mu}_i^{\text{G}^\pm} - \bar{\mu}_i^{\text{G}'}) \langle \psi | \bar{f}_i^{\text{el}} | \psi \rangle - \frac{1}{2} \sum_i (\bar{\mu}_i^{\text{G}} - \bar{\mu}_i^{\text{G}'}) \bar{F}_i^{\text{tot,G}} \right) \quad (29)$$

$$\Delta E = \left( W_1^{\text{EX}} + \frac{1}{2} \sum_i (\bar{\mu}_i^{\text{G}} - \bar{\mu}_i^{\text{G}'}) \langle \psi_{\text{CIS}} | \bar{f}_i^{\text{el}} | \psi_{\text{CIS}} \rangle \right) - \left( W^{\text{G}} + \frac{1}{2} \sum_i (\bar{\mu}_i^{\text{G}} + \bar{\mu}_i^{\text{G}^\pm} - \bar{\mu}_i^{\text{G}'}) \langle \psi | \bar{f}_i^{\text{el}} | \psi \rangle \right) \quad (30)$$

**Method 2.** In method 2, an excited-state energy is obtained by including the ground-state solvent-induced dipole terms as described in the formulation of method 1; then, once the iterative process is complete, a one-time correction term is added to account for the solvent response for the excited-state density. This is accomplished by recalculating the induced dipoles corresponding to the excited-state density.

The method 1 eqs 21–24 also apply to method 2. They lead to the method 2 quantum mechanical energy in analogy with eq 24

$$W_2^{\text{EX}} = E_0^{\text{EX}} - \frac{1}{2} \sum_i (\bar{\mu}_i^{\text{G}} - \bar{\mu}_i^{\text{G}'}) \langle \psi_{\text{CIS}} | \bar{f}_i^{\text{el}} | \psi_{\text{CIS}} \rangle \quad (31)$$

where  $W_2^{\text{EX}}$  is the method 2 quantum mechanical energy.

Since the application of the variational method does not provide the complete polarization energy contribution, the total energy of the hybrid QM/MM system is (see eq 25)

$$E_2^{\text{EX}} = E_0^{\text{EX}} + E_{\text{pol}}^{\text{EX}} \quad (32)$$

where  $E_{\text{pol}}^{\text{EX}}$  is the polarization energy for the excited state (eq 7). Therefore (see eq 27)

$$E_2^{\text{EX}} = W_2^{\text{EX}} + \frac{1}{2} \sum_i (\bar{\mu}_i^{\text{G}} - \bar{\mu}_i^{\text{G}'}) \langle \psi_{\text{CIS}} | \bar{f}_i^{\text{el}} | \psi_{\text{CIS}} \rangle - \frac{1}{2} \sum_i (\bar{\mu}_i^{\text{EX}} - \bar{\mu}_i^{\text{EX}'}) \bar{F}_i^{\text{tot,EX}} \quad (33)$$

Equation 33 contains the explicit polarization response to the excited-state density, unlike method 1 in which no explicit polarization response is added to the excited state.

The solvated QM excited-state energy obtained using method 1 contains the ground-state induced dipole terms (eq 31), and in principle, the excited-state energy could be formulated using eq 6. Therefore, a correction term that accounts for the interaction of the ground-state dipoles and the excited-state wave function must be added to  $W_2^{\text{EX}}$  in method 2. This correction term is

$$\langle \psi_{\text{CIS}} | H_0^{\text{EX}} + H_{\text{pol}}^{\text{EX}} | \psi_{\text{CIS}} \rangle - \langle \psi_{\text{CIS}} | H_0^{\text{EX}} + H_{\text{pol}}^{\text{G}} | \psi_{\text{CIS}} \rangle \quad (34)$$

The second term in eq 34 corresponds to the second term in eq 31, which is the ground-state induced dipole term. The first term

in eq 34 adds the electron polarization response to the excited-state dipoles.

The leading correction term in eq 34 can be simplified to

$$= -\left(\frac{1}{2} \sum_i [(\vec{\mu}_i^{\text{EX}} - \vec{\mu}_i^{\text{EX}'}) - (\vec{\mu}_i^{\text{G}} - \vec{\mu}_i^{\text{G}'})] \langle \langle \psi_{\text{CIS}} | \vec{f}_i^{\text{el}} | \psi_{\text{CIS}} \rangle \rangle \right) \quad (35)$$

Adding the correction term (eq 35) to eq 33

$$E_2^{\text{EX}} = W_2^{\text{EX}} + \frac{1}{2} \sum_i (\vec{\mu}_i^{\text{G}} - \vec{\mu}_i^{\text{G}'}) \langle \psi_{\text{CIS}} | \vec{f}_i^{\text{el}} | \psi_{\text{CIS}} \rangle - \frac{1}{2} \sum_i (\vec{\mu}_i^{\text{EX}} - \vec{\mu}_i^{\text{EX}'}) \vec{F}_i^{\text{tot,EX}} - \left( \frac{1}{2} \sum_i [(\vec{\mu}_i^{\text{EX}} - \vec{\mu}_i^{\text{EX}'}) - (\vec{\mu}_i^{\text{G}} - \vec{\mu}_i^{\text{G}'})] \langle \langle \psi_{\text{CIS}} | \vec{f}_i^{\text{el}} | \psi_{\text{CIS}} \rangle \rangle \right) \quad (36)$$

Equation 36 can be written in the form of eq 27 as

$$W_1^{\text{EX}} + \frac{1}{2} \sum_i (\vec{\mu}_i^{\text{G}} - \vec{\mu}_i^{\text{G}'}) \langle \psi_{\text{CIS}} | \vec{f}_i^{\text{el}} | \psi_{\text{CIS}} \rangle = E_1^{\text{EX}} + \frac{1}{2} \sum_i (\vec{\mu}_i^{\text{G}} - \vec{\mu}_i^{\text{G}'}) \vec{F}_i^{\text{tot,G}} \quad (37)$$

Using  $W_1^{\text{EX}} = W_2^{\text{EX}}$  and eq 37, eq 36 becomes

$$E_2^{\text{EX}} = E_1^{\text{EX}} + \frac{1}{2} \sum_i (\vec{\mu}_i^{\text{G}} - \vec{\mu}_i^{\text{G}'}) \vec{F}_i^{\text{tot,G}} - \frac{1}{2} \sum_i (\vec{\mu}_i^{\text{EX}} - \vec{\mu}_i^{\text{EX}'}) \vec{F}_i^{\text{tot,EX}} - \left( \frac{1}{2} \sum_i [(\vec{\mu}_i^{\text{EX}} - \vec{\mu}_i^{\text{EX}'}) - (\vec{\mu}_i^{\text{G}} - \vec{\mu}_i^{\text{G}'})] \langle \langle \psi_{\text{CIS}} | \vec{f}_i^{\text{el}} | \psi_{\text{CIS}} \rangle \rangle \right) \quad (38)$$

Equation 38 is the final working equation for method 2. Note that the response to the excited-state density is not fully iterated to self-consistency.

The three methods described here are general approaches and can be applied to other QM methods as well.

### III. Computational Methods

Solvent-induced shifts are calculated by taking the difference between the gas-phase and aqueous-phase vertical excitation energies of the solute. Several examples are used to test the CIS/EFP1 method, a water dimer ( $\text{H}_2\text{O}(\text{H}_2\text{O})$ ), formaldehyde with 1 water ( $\text{HCHO}(\text{H}_2\text{O})$ ), dimethyl sulphoxide in 4 waters ( $\text{CH}_3\text{SOCH}_3(\text{H}_2\text{O})_4$ ), and dimethyl sulphoxide in 14 waters ( $\text{CH}_3\text{SOCH}_3(\text{H}_2\text{O})_{14}$ ). The solute molecules in these examples are treated using the CIS method, and the water molecules are described with the EFP1/HF method. The ground-state structures are optimized using RHF/6-31G+(d,p), and the vertical excitation energies are calculated using the CIS/EFP methods 1 and 2 described in the previous section. The solvent-induced shifts calculated in this manner are compared with full ab initio calculations, in which both the solute and the solvent molecules are treated using the CIS/6-31+G(d) level of theory at the same geometry as that for CIS/EFP1.

In addition to the test examples discussed in the previous paragraph, the CIS/EFP1 method 1 was also used to calculate the solvent-induced shifts of solute molecules in bulk solution.

**TABLE 1: Vertical Excitation Energies ( $n \rightarrow \pi^*$ ) and Solvent-Induced Shifts (eV) for HCHO( $\text{H}_2\text{O}$ ) Calculated Using CIS/EFP Methods 1 and 2 and with Full Ab Initio CIS**

	method 1	method 2	full CIS
vertical excitation energy ( $\Delta E$ )	4.87	4.86	4.87
solvent shift <sup>a</sup>	0.18	0.17	0.18

<sup>a</sup> The gas-phase vertical excitation energy is 4.69 eV.

**TABLE 2: Vertical Excitation Energies ( $n \rightarrow \sigma^*$ ) and Solvent-Induced Shifts (eV) for  $\text{H}_2\text{O}(\text{H}_2\text{O})$  Calculated using CIS/EFP1 methods 1 and 2 and with Full Ab Initio CIS**

	method 1	method 2	full CIS
vertical excitation energy ( $\Delta E$ )	9.75	9.72	9.71
solvent shift <sup>a</sup>	0.42	0.39	0.38

<sup>a</sup> The gas-phase vertical excitation energy is 9.33 eV.

**TABLE 3: Vertical Excitation Energies ( $n \rightarrow \sigma^*$ ) and Solvent-Induced Shifts (eV) for  $\text{CH}_3\text{SOCH}_3(\text{H}_2\text{O})_4$  calculated using CIS/EFP1 Methods 1 and 2 and with Full Ab Initio CIS**

	method 1	method 2	full CIS
vertical excitation energy ( $\Delta E$ )	7.06	7.05	7.06
solvent shift <sup>a</sup>	0.16	0.16	0.17

<sup>a</sup> The gas-phase vertical excitation energy is 6.89 eV.

Two systems, acetone in 100 EFP1 water molecules and coumarin 151 in 150 EFP1 waters, were chosen to study the solvent-induced shifts in the condensed phase. For both systems, the molecular dynamics (MD) method was employed to generate several configurations. In the MD simulations, an isolated system consisted of 100 EFP1 waters with 1 acetone molecule and 150 EFP1 water molecules with 1 coumarin 151 molecule. For both systems, acetone and coumarin 151 belong to the QM region, and the EFP1 water molecules belong to the MM region. A Nosé–Hoover chain method<sup>65</sup> was employed to perform the canonical ensemble (NVT) simulation at 300 K temperature, and a 1 fs time step was chosen. The data was obtained from equilibrated trajectories of 3–6 ps length, during which the snapshots were taken at every 10 fs. At each snapshot, the vertical excitation energy was calculated using the CIS/EFP1 method 1. The EFP internal geometries were frozen, but there were no such restrictions on the internal solute structures. All calculations were done using electronic structure code GAMESS.<sup>66</sup> The structures shown in the figures are visualized with a graphical interface to GAMESS called MacMolPlot.<sup>67</sup>

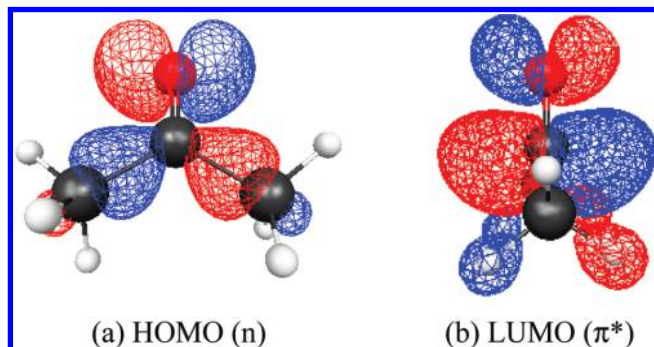
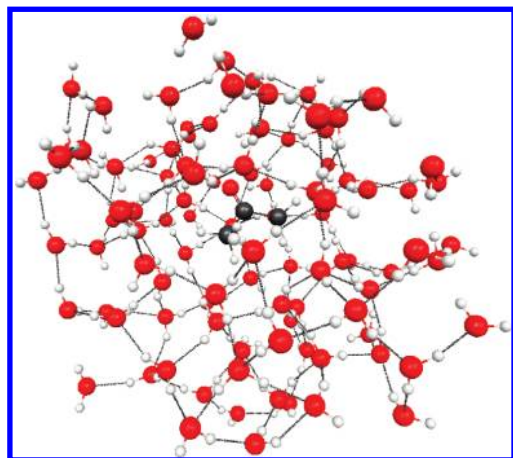
### IV. Results and Discussion

Tables 1–4 show the vertical excitation energies and the solvent-induced shifts calculated using CIS/EFP1 methods 1 and 2. The solvent-induced shifts of formaldehyde plus one water are examined in Table 1. The shifts calculated using both methods 1 and 2 are in very good agreement with the full ab initio values. The same is true for the water dimer shown in Table 2, dimethyl sulphoxide( $\text{H}_2\text{O}$ )<sub>4</sub> in Table 3, and  $\text{CH}_3\text{SOCH}_3(\text{H}_2\text{O})_{14}$  in Table 4. In all examples, the errors are on the order of a few hundredths of an eV. The accuracy of method 1 relative to that of method 2 and to that of the full QM results for both absolute excitation energies and solvent shifts suggests that at least for these four test molecules, the indirect effect of the perturbation of the ground-state molecular orbitals by the EFP1 potential makes the overwhelming

**TABLE 4: Vertical Excitation Energies ( $n \rightarrow \pi^*$ ) and Solvent-Induced Shifts (eV) for  $\text{CH}_3\text{SOCH}_3(\text{H}_2\text{O})_{14}$  Calculated using CIS/EFP1 Methods 1 and 2 and with Full Ab Initio CIS**

	method 1	method 2	full CIS
vertical excitation energy ( $\Delta E$ )	7.29	7.28	7.30
solvent shift <sup>a</sup>	0.50	0.49	0.51

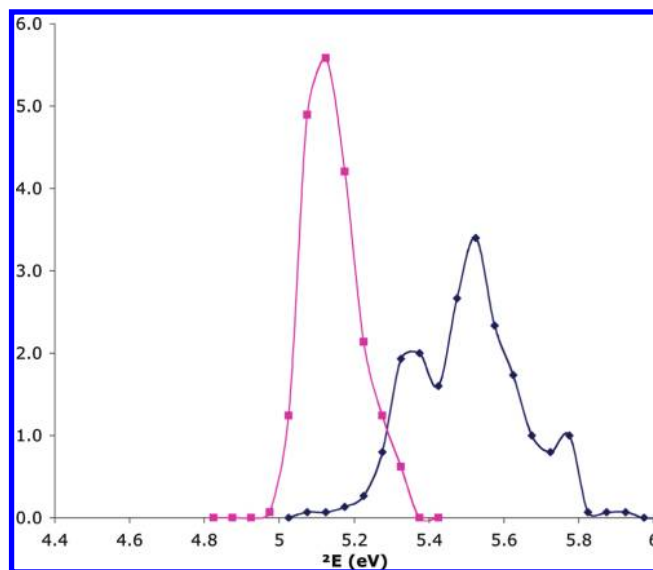
<sup>a</sup> The gas-phase vertical excitation energy is 6.79 eV.

**Figure 1.** The highest occupied (a) and lowest unoccupied (b) molecular orbitals of acetone ( $\text{CH}_3\text{COCH}_3$ ).**Figure 2.** A snapshot of acetone in 100 EFP1 water molecules during the molecular dynamics simulation.

contribution to the solvent-induced shifts. In comparison, the perturbation of the excited-state wave function has only a very minor effect. This may not always be the case, and many more examples must be tested with CIS and more sophisticated excited-state methods. However, a tentative conclusion is that the fully consistent method is not expected to be required. Consequently, in the next two examples, only method 1 is considered. Method 1 is now applied to study acetone in 100 EFP1 water molecules and coumarin 151 in 150 EFP1 waters.

**Acetone in 100 EFP1.** The absorption of acetone has been extensively studied in previous theoretical calculations<sup>30,50,68,69</sup> as well as in experimental measurements.<sup>70–72</sup> The  $S_0$  to  $S_1$  excitation in acetone is the  $n \rightarrow \pi^*$  excitation that occurs from an O lone pair into the  $\pi^*$  orbital of the carbonyl double bond. The highest occupied ( $n$ ) and lowest unoccupied ( $\pi^*$ ) molecular orbitals are shown in Figure 1.

MD simulations were used to generate several configurations of acetone in 100 EFP1 water molecules at 300 K. A snapshot of acetone in 100 EFP1 waters during a MD simulation is shown in Figure 2. A simulated absorption spectrum was generated by calculating the vertical excitation energy at each snapshot obtained from the MD simulation. Simulated absorption spectra

**Figure 3.** A simulated spectrum for the  $n \rightarrow \pi^*$  vertical excitation energy of acetone. The curve on the left is for gas-phase acetone, and the one on the right is for solvated acetone.**TABLE 5: Comparison of the Calculated Average Vertical Excitation Energies ( $n \rightarrow \pi^*$ ) and Solvent-Induced Shifts (eV) of Acetone in the Gas and Aqueous Phases with Those from Previous Work**

	Gas Phase		
	expt <sup>70–72</sup>	TDDFT <sup>30</sup>	CIS
vertical excitation energy ( $\Delta E$ )	4.48	4.38	5.16
	Aqueous Phase		
	expt <sup>70–72</sup>	TDDFT/EFP1 <sup>30</sup>	method 1
vertical excitation energy ( $\Delta E$ )	4.67–4.69	4.59	5.52
solvent shift	0.19–0.21	0.21	0.36

of the acetone molecule in both the gas and aqueous phases are shown in Figure 3. The curve on the left illustrates the gas-phase  $n \rightarrow \pi^*$  absorption spectrum, while the one on the right shows the absorption spectrum for solvated acetone. The calculated acetone spectrum shows a solvent-induced blue shift for the  $n \rightarrow \pi^*$ ; this is qualitatively consistent with the experimental results.<sup>72</sup> The averaged gas-phase and aqueous-phase acetone  $n \rightarrow \pi^*$  vertical excitation energies and solvent-induced shifts are compared in Table 5 with previous experimental measurements<sup>70,71</sup> and theoretical calculations.<sup>30</sup> The CIS/EFP1 vertical excitation energies are overestimated, reflecting the approximate nature of the CIS method; however, the solvent-induced shifts in the absorption spectrum predicted by CIS/EFP1 are in qualitative agreement with the previous results.

**Coumarin 151 in 150 EFP waters.** Coumarins have been studied extensively because they are known to exhibit desirable anticancer and antibiotic properties.<sup>73,74</sup> They also exhibit interesting solvent dynamics.<sup>4,9,75,76</sup> There have been several experimental and theoretical studies of the excited-state properties of coumarin 151.<sup>19,69,77–79</sup> The  $\pi \rightarrow \pi^*$  transition in the gas and condensed phases of the coumarin 151 molecule is studied here. The HOMO ( $\pi$ ) and LUMO ( $\pi^*$ ) coumarin 151 orbitals are shown in Figure 4. Simulated  $\pi \rightarrow \pi^*$  absorption spectra in the gas and condensed phases were generated using several configurations obtained from MD simulations at 300 K (see Figure 5). A snapshot of coumarin 151 in 150 EFP waters during

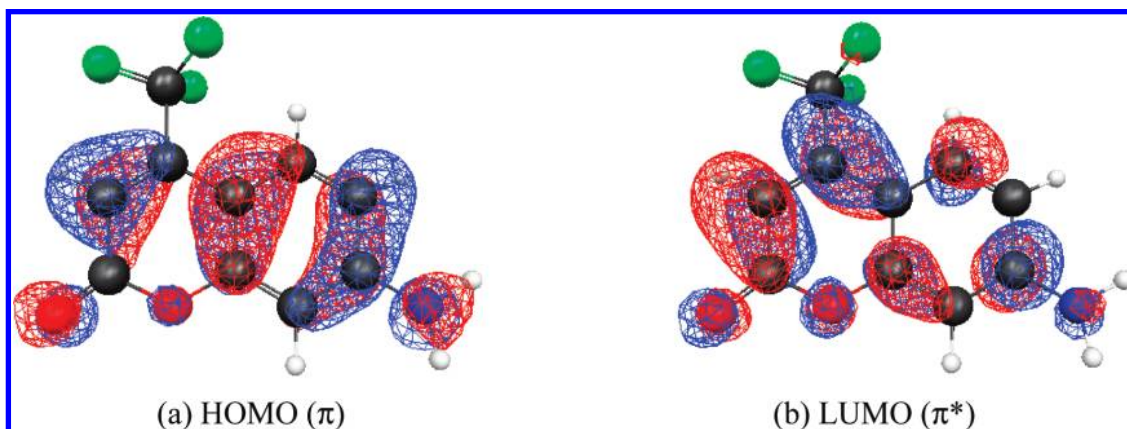


**Figure 4.** (a) The highest occupied ( $\pi$ ) and (b) lowest unoccupied ( $\pi^*$ ) molecular orbitals of coumarin 151 (7-amino-4-trifluoromethyl-1,2-benzopyrone).

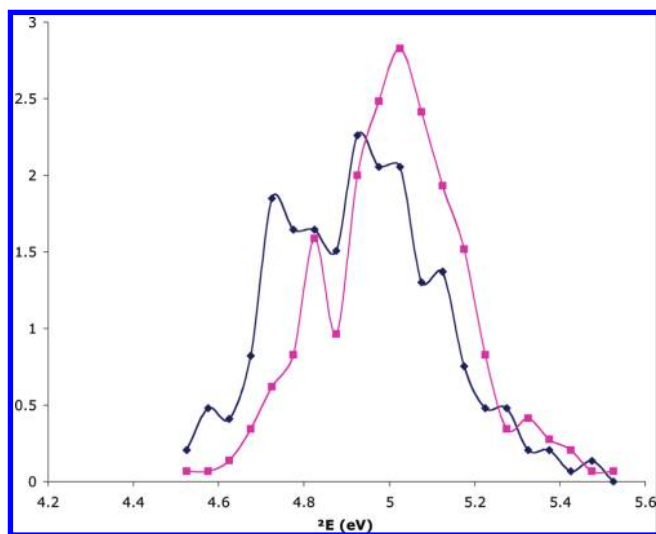


**Figure 5.** A simulated spectrum for a  $\pi \rightarrow \pi^*$  vertical excitation energy of coumarin 151. The right curve is for the gas-phase coumarin 151, and the left curve represents the solvated coumarin 151.

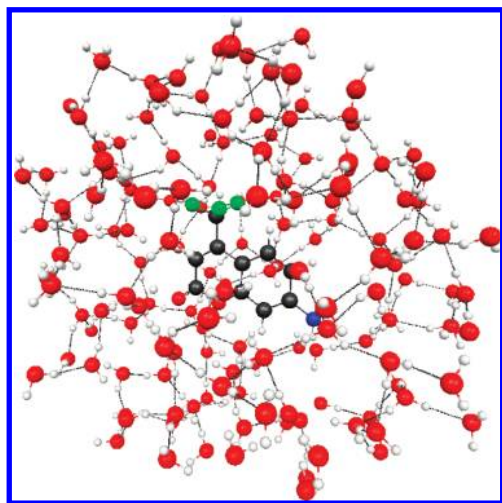


**Figure 6.** A snapshot of coumarin 151 in 150 EFP1 water molecules during a molecular dynamics simulation.

the MD simulation is shown in Figure 6. The averaged  $\pi \rightarrow \pi^*$  vertical excitation energies in the gas and aqueous phases are compared with experimental values in Table 6. The CIS/EFP1 method overestimates the vertical excitation energies relative to the experiments, as one would expect. However, a red shift is correctly predicted for the  $\pi \rightarrow \pi^*$  excitation of coumarin

**TABLE 6: Comparison of the Average Vertical Excitation Energy ( $\pi \rightarrow \pi^*$ ) and Solvent Shifts (eV) of Coumarin 151 in the Gas and Aqueous Phases with Those from Previous Experimental Work**

	expt <sup>77</sup> (gas)	expt <sup>69</sup> (aqueous)	CIS (gas)	method 1
vertical excitation energy ( $\Delta E$ )	3.55	3.48	4.99	4.91
solvent shift		0.08		0.07

151 as the medium is changed from the gas to aqueous phase; this is qualitatively consistent with previous experimental and theoretical calculations.<sup>13,43,47,55,68–75</sup>

## V. Conclusions

In order to study the solvent-induced shifts in the electronic spectra, the work herein discusses three approaches that have been formulated to interface a QM method for excited states (CIS) with an explicit solvent method called EFP. The main question that has been addressed in this study is how to incorporate the polarization perturbation due to the solvent molecules in the excited-state energy.

The fully self-consistent method is the most sophisticated and complex approach that calculates the solvent response within the CIS iterative procedure to obtain an excited state that is fully consistent with the environment. The second approach, method 1, is the simplest approach that indirectly alters the excited states via HF orbitals that are modified due to their interactions with the EFP solvent molecules. The third approach (method 2) is an approximation to the fully self-consistent method and adds a one-time perturbative correction term that includes the solvent response for the excited-state density. Methods 1 and 2 have been implemented and successfully tested in GAMESS for microsolvated solute molecules. The test examples examined here show that both methods 1 and 2 predict vertical excitation energies and solvent shifts that are in good agreement with the full ab initio results. The accuracy of method 1 relative to the full QM results leads to the conclusion that the indirect effect of the perturbation of the ground-state molecular orbitals by the EFP1 potential makes by far the most significant contribution to the solvent-induced shifts. Indeed, the modifications in method 2 relative to method 1 have a very small impact on the solvent-induced shifts. The CIS/EFP1 method 1, as applied to the prediction of bulk solvent effects on the vertical excitation energies of acetone and coumarin 151, exhibits qualitative agreement with the experimental measurements.



Therefore, method 1 is a simple method that can be employed to semiquantitatively study solvent effects in large systems.

It is important to recognize that the formulations described here to combine the excited-state method, CIS, with the explicit solvent model, EFP1, are general and can therefore be extended to more sophisticated excited-state methods, such as EOM-CC, multireference CI, multireference perturbation theory, and CISD, to accurately capture the quantitative solvent effects on the excited states.

**Acknowledgment.** This research was supported by a grant (to M.S.G.) from the U.S. Department Of Energy, Office of Science, Basic Energy Sciences, administered by the Ames Laboratory, Iowa State University, and by support (to L.V.S.) from Purdue University, the Petroleum Research Fund (49271-DNI6) and the National Science Foundation (CHE-0955419). The authors gratefully acknowledge helpful discussions with Drs. Michael W. Schmidt and Paul N. Day.

## References and Notes

- Chapman, C. F.; Maroncelli, M. *J. Phys. Chem.* **1991**, *95*, 9095.
- Chowdhury, P. K.; Halder, M.; Sanders, L.; Arnold, R. A.; Liu, Y.; Armstrong, D. W.; Kundu, S.; Hargrove, M. S.; Song, X.; Petrich, J. W. *Photochem. Photobiol.* **2004**, *79*, 440.
- Chapman, C. F.; Fee, R. S.; Maroncelli, M. *J. Phys. Chem.* **1990**, *94*, 4929.
- Jimenez, R.; Fleming, G. R.; Kumar, P. V.; Maroncelli, M. *Nature* **1994**, *369*, 471.
- Rechthaler, K.; Kohler, G. *Chem. Phys.* **1994**, *189*, 99.
- Jones, G.; Feng, Z. M.; Bergmark, W. R. *J. Phys. Chem.* **1994**, *98*, 4511.
- Jones, G.; Jackson, W. R.; Choi, C.; Bergmark, W. R. *J. Phys. Chem.* **1985**, *89*, 294.
- Zhao, W. W.; Pan, L.; Bian, W. S.; Wang, J. P. *ChemPhysChem* **2008**, *9*, 1593.
- Hornig, M. L.; Gardecki, J. A.; Papazyan, A.; Maroncelli, M. *J. Phys. Chem.* **1995**, *99*, 17311.
- Adhikary, R.; Barnes, C. A.; Petrich, J. W. *J. Phys. Chem. B* **2009**, *113*, 11999.
- Chowdhury, P. K.; Halder, M.; Sanders, L.; Calhoun, T.; Anderson, J. L.; Armstrong, D. W.; Song, X.; Petrich, J. W. *J. Phys. Chem. B* **2004**, *108*, 10245.
- Halder, M.; Headley, L. S.; Mukherjee, P.; Song, X.; Petrich, J. W. *J. Phys. Chem. A* **2006**, *110*, 8623.
- Pal, S. K.; Zewail, A. H. *Chem. Rev.* **2004**, *104*, 2099.
- Bose, S.; Adhikary, R.; Mukherjee, P.; Song, X. Y.; Petrich, J. W. *J. Phys. Chem. B* **2009**, *113*, 11061.
- Bauernschmitt, R.; Ahlrichs, R. *Chem. Phys. Lett.* **1996**, *256*, 454.
- Bauernschmitt, R.; Haser, M.; Treutler, O.; Ahlrichs, R. *Chem. Phys. Lett.* **1997**, *264*, 573.
- Miertus, S.; Scrocco, E.; Tomasi, J. *Chem. Phys.* **1981**, *55*, 117.
- Karelson, M.; Zerner, M. C. *J. Am. Chem. Soc.* **1990**, *112*, 9405.
- Cave, R. J.; Burke, K.; Castner, E. W. *J. Phys. Chem. A* **2002**, *106*, 9294.
- Karelson, M. M.; Katritzky, A. R.; Zerner, M. C. *Int. J. Quantum Chem.* **1986**, 521.
- Chipman, D. M. *Theor. Chem. Acc.* **2002**, *107*, 80.
- Tomasi, J.; Persico, M. *Chem. Rev.* **1994**, *94*, 2027.
- Tomasi, J.; Mennucci, B.; Cammi, R. *Chem. Rev.* **2005**, *105*, 2999.
- Karelson, M. M.; Zerner, M. C. *J. Phys. Chem.* **1992**, *96*, 6949.
- Li, J.; Cramer, C. J.; Truhlar, D. G. *Int. J. Quantum Chem.* **2000**, *77*, 264.
- Cossi, M.; Barone, V. *J. Chem. Phys.* **2000**, *112*, 2427.
- Minezawa, N.; Kato, S. *J. Chem. Phys.* **2007**, 126.
- Gordon, M. S.; Freitag, M. A.; Bandyopadhyay, P.; Jensen, J. H.; Kairys, V.; Stevens, W. J. *J. Phys. Chem. A* **2001**, *105*, 293.
- Day, P. N.; Jensen, J. H.; Gordon, M. S.; Webb, S. P.; Stevens, W. J.; Krauss, M.; Garmer, D.; Basch, H.; Cohen, D. *J. Chem. Phys.* **1996**, *105*, 1968.
- Yoo, S.; Zahariev, F.; Sok, S.; Gordon, M. S. *J. Chem. Phys.* **2008**, 129.
- Foresman, J. B.; Headgordon, M.; Pople, J. A.; Frisch, M. J. *J. Phys. Chem.* **1992**, *96*, 135.
- Tuck, P. O.; Mawhinney, R. C.; Rappon, M. *Phys. Chem. Chem. Phys.* **2009**, *11*, 4471.
- Sanchez, M. L.; Aguilar, M. A.; Delvalle, F. J. O. *J. Phys. Chem.* **1995**, *99*, 15758.
- Kina, D.; Arora, P.; Nakayama, A.; Noro, T.; Gordon, M. S.; Taketsugu, T. *Int. J. Quantum Chem.* **2009**, *109*, 2308.
- Krauss, M.; Webb, S. P. *J. Chem. Phys.* **1997**, *107*, 5771.
- Kina, D.; Nakayama, A.; Noro, T.; Taketsugu, T.; Gordon, M. S. *J. Phys. Chem. A* **2008**, *112*, 9675.
- Besley, N. A.; Hirst, J. D. *J. Am. Chem. Soc.* **1999**, *121*, 8559.
- Parusel, A. B. J.; Rettig, W.; Sudholt, W. *J. Phys. Chem. A* **2002**, *106*, 804.
- Nakatsuji, H.; Hirao, K. *Chem. Phys. Lett.* **1977**, *47*, 569.
- Miyahara, T.; Nakatsuji, H.; Hasegawa, J.; Osuka, A.; Aratani, N.; Tsuda, A. *J. Chem. Phys.* **2002**, *117*, 11196.
- Geertsen, J.; Rittby, M.; Bartlett, R. J. *Chem. Phys. Lett.* **1989**, *164*, 57.
- Fan, P. D.; Valiev, M.; Kowalski, K. *Chem. Phys. Lett.* **2008**, *458*, 205.
- Kowalski, K.; Piecuch, P. *J. Chem. Phys.* **2004**, *120*, 1715.
- Kawashima, Y.; Hashimoto, T.; Nakano, H.; Hirao, K. *Theor. Chem. Acc.* **1999**, *102*, 49.
- Nakayama, K.; Nakano, H.; Hirao, K. *Int. J. Quantum Chem.* **1998**, *66*, 157.
- Xu, Z. R.; Matsika, S. *J. Phys. Chem. A* **2006**, *110*, 12035.
- Kistler, K. A.; Matsika, S. *J. Phys. Chem. A* **2009**, *113*, 12396.
- Jensen, J. H.; Gordon, M. S. *J. Chem. Phys.* **1998**, *108*, 4772.
- Adamovic, I.; Gordon, M. S. *Mol. Phys.* **2005**, *103*, 379.
- Aidas, K.; Kongsted, J.; Osted, A.; Mikkelsen, K. V.; Christiansen, O. *J. Phys. Chem. A* **2005**, *109*, 8001.
- Kongsted, J.; Osted, A.; Mikkelsen, K. V.; Christiansen, O. *J. Chem. Phys.* **2003**, *118*, 1620.
- Warshel, A. *J. Phys. Chem.* **1979**, *83*, 1640.
- Luzhkov, V.; Warshel, A. *J. Am. Chem. Soc.* **1991**, *113*, 4491.
- Thompson, M. A.; Schenter, G. K. *J. Phys. Chem.* **1995**, *99*, 6374.
- Gao, J. L.; Byun, K. *Theor. Chem. Acc.* **1997**, *96*, 151.
- Tapia, O.; Goscinski, O. *Mol. Phys.* **1975**, *29*, 1653.
- Davidson, E. R. *J. Comput. Phys.* **1975**, *17*, 87.
- Adamovic, I.; Freitag, M. A.; Gordon, M. S. *J. Chem. Phys.* **2003**, *118*, 6725.
- Stone, A. J. *Chem. Phys. Lett.* **1981**, *83*, 233.
- Slipchenko, L. V.; Gordon, M. S. *Mol. Phys.* **2009**, *107*, 999.
- Feynman, R. P. *Phys. Rev.* **1939**, *56*, 340.
- Gerratt, J.; Mills, I. M. *J. Chem. Phys.* **1968**, *49*, 1730.
- Gerratt, J.; Mills, I. M. *J. Chem. Phys.* **1968**, *49*, 1719.
- DeFusco, A.; Schmidt, M. W.; Ivanic, J.; Gordon, M. S. In preparation.
- Martyna, G. J.; Tuckerman, M. E.; Tobias, D. J.; Klein, M. L. *Mol. Phys.* **1996**, *87*, 1117.
- Gordon, M. S.; Schmidt, M. W. In *Theory and Applications of Computational Chemistry: The First Forty Years*, Dykstra, C. E., Frenking, G., Kinn, K. S., Scuseria, G. E.; Eds. Elsevier: Amsterdam, The Netherlands, 2005.
- Bode, B. M.; Gordon, M. S. *J. Mol. Graphics Modell.* **1998**, *16*, 133.
- Rohrig, U. F.; Frank, I.; Hutter, J.; Laio, A.; VandeVondele, J.; Rothlisberger, U. *ChemPhysChem* **2003**, *4*, 1177.
- Sulpizi, M.; Rohrig, U. F.; Hutter, J.; Rothlisberger, U. *Int. J. Quantum Chem.* **2005**, *101*, 671.
- Bayliss, N. S.; McRae, E. G. *J. Phys. Chem.* **1954**, *58*, 1006.
- Bayliss, N. S.; Will-Johnson, G. *Spectrochim. Acta, Part A* **1968**, *A 24*, 551.
- Hayes, W. P.; Timmons, C. J. *Spectrochim. Acta* **1965**, *21*, 529.
- Singer, K. D.; Lalama, S. L.; Sohn, J. E.; Small, R. D. *Nonlinear Optical Properties of Organic Molecules and Crystals*; Academic Press: Orlando, FL, 1987; Chapter II-8.
- Nicoud, J. F.; Twieg, R. J. *Nonlinear Optical Properties of Organic Molecules and Crystals*; Academic Press: Orlando, FL, 2002; Chapter II-3.
- Chowdhury, P. K.; Halder, M.; Sanders, L.; Arnold, R. A.; Liu, Y.; Armstrong, D. W.; Kundu, S.; Hargrove, M. S.; Song, X.; Petrich, J. W. *Photochem. Photobiol.* **2004**, *79*, 440.
- Halder, M.; Mukherjee, P.; Bose, S.; Hargrove, M. S.; Song, X. Y.; Petrich, J. W. *J. Chem. Phys.* **2007**, 127.
- Pryor, B. A.; Palmer, P. M.; Andrews, P. M.; Berger, M. B.; Topp, M. R. *J. Phys. Chem. A* **1998**, *102*, 3284.
- Sulpizi, M.; Carloni, P.; Hutter, J.; Rothlisberger, U. *Phys. Chem. Chem. Phys.* **2003**, *5*, 4798.
- Neugebauer, J.; Jacob, C. R.; Wesolowski, A. T.; Baerends, E. J. *J. Phys. Chem.* **2005**, *109*, 7805.